

# Soil infiltration characteristics and pore distribution under freezing-thawing conditions

Ruiqi Jiang<sup>1,2,3,\*</sup>, Tianxiao Li<sup>1,2,3,\*</sup>, Dong Liu<sup>1,2,3,\*</sup>, Qiang Fu<sup>1,2,3,\*</sup>, Renjie Hou<sup>1,2,3</sup>,  
Qinglin Li<sup>1</sup>, Song Cui<sup>1,2,3</sup>, Mo Li<sup>1,2,3</sup>

<sup>1</sup> School of Water Conservancy & Civil Engineering, Northeast Agricultural University, Harbin 150030, China

<sup>2</sup> Key Laboratory of Effective Utilization of Agricultural Water Resources of Ministry of Agriculture, Northeast Agricultural University, Harbin, Heilongjiang 150030, China

<sup>3</sup> Heilongjiang Provincial Key Laboratory of Water Resources and Water Conservancy Engineering in Cold Region, Northeast Agricultural University, Harbin, Heilongjiang 150030, China

\* Dong Liu and Qiang Fu are corresponding authors.

★ These authors contributed equally to this work.

\*Corresponding author at: School of Water Conservancy and Civil Engineering, Northeast Agricultural University, Harbin, Heilongjiang 150030, China

Correspondence to: [liudong9599@yeah.net](mailto:liudong9599@yeah.net) (Dong Liu). [fuqiang0629@126.com](mailto:fuqiang0629@126.com) (Qiang Fu)

**Abstract.** Frozen soil infiltration widely occurs in hydrological processes such as seasonal soil freezing and thawing, snowmelt infiltration, and runoff. Accurate measurement and simulation of parameters related to frozen soil infiltration processes are highly important for agricultural water management, environmental issues and engineering problems in cold regions. Temperature changes cause soil pore size distribution variations and consequently dynamic infiltration capacity changes during different freeze-thaw periods. To better understand these complex processes and to reveal the freeze-thaw action effects on soil pore distribution and infiltration capacity, ~~selected~~ black soils, ~~and~~ meadow soils and chernozem were selected as test subjects, these soil types ~~which~~ account for the largest arable land area in Heilongjiang Province, China.

24 Laboratory tests of soils at different temperatures were conducted using a tension infiltrometer and ethylene  
25 glycol aqueous solution. The stable infiltration rate, ~~and~~ hydraulic conductivity were measured, and the  
26 soil pore distribution was calculated. The results indicated that for the different soil types, macropores, which  
27 constituted approximately 0.1% to 0.2% of the soil volume under unfrozen conditions, contributed  
28 approximately 50% of the saturated flow, and after soil freezing, the soil macropore proportion decreased to  
29 0.05% to 0.1%, while the ~~the~~ saturated flow proportion decreased to approximately 30%. Soil moisture froze  
30 into ice crystals inside relatively large pores, resulting in numerous smaller-sized pores, which reduced the  
31 number of macropores ~~while~~ ~~but~~ ~~increas~~ ~~eding~~ the number of smaller-sized mesopores, so that the frozen soil  
32 infiltration capacity was no longer solely dependent on the macropores. After the ice crystals had melted,  
33 more pores were formed within the soil, enhancing the soil permeability.

34 **Key words:** Freezing-thawing soil; Hydraulic conductivity; Pore distribution; Macropores; Infiltration  
35 characteristics

## 36 **1 Introduction**

37 Over the last few decades, the temperature changes caused by global warming have altered the freezing state  
38 of near-surface soils, and in China, changes in characteristic values such as the extent of the mean annual  
39 area ~~extent of the~~ seasonal soil freeze/thaw state and maximum freezing depth, indicate the degradation of  
40 frozen soil, especially at high latitudes (Wang et al., 2019; Peng et al., 2016). Under the effect of temperature,  
41 most frozen regions experience ~~the~~ seasonal freezing and thawing of soil, accompanied by coupled soil water  
42 and heat movement ~~and~~ as well as frost heave processes, thus making the soil structure and function more  
43 variable (Oztas and Fayetorbay, 2003; Fu et al., 2019; Gao et al., 2018). Parameters such as the soil infiltration  
44 rate and hydraulic conductivity are key factors in the study of soil water movement, groundwater recharge,  
45 and solute and contaminant transport simulation (Angulo-Jaramillo et al., 2000). In regard to unfrozen soils,

46 ~~the~~ temperature has been shown to change the soil structure and kinematic viscosity of soil water, thereby  
47 affecting the unsaturated hydraulic conductivity of soils (Gao and Shao, 2015). In terms of frozen soils, the  
48 water infiltration characteristics and pore size distribution are highly variable and difficult to observe  
49 (Watanabe et al., 2013); moreover, the water movement in freezing-thawing soils is complicated by the  
50 migration of water and heat and the associated water phase change (~~Jarvis et al., 2016~~; Hayashi, 2013). The  
51 accurate measurement of water movement parameters and soil pore distribution under freeze-thaw  
52 conditions is a necessary prerequisite for the quantitative description of the water movement in frozen soil,  
53 and the mechanism and degree of influence of the temperature on the infiltration rate, hydraulic conductivity,  
54 porosity and other parameters in the different stages of freeze-thaw periods require further research.

55 Currently, ~~the studies related to the~~ quantitative ~~studies characterization~~ of the infiltration process in freezing-  
56 thawing soils ~~infiltration~~ can be mainly divided into experimental and model studies. Field experiments have  
57 been performed less often because under natural conditions, ~~the~~ infiltration water ~~establishes~~ exhibits a  
58 preferential flow into the deep soil, and the alternating freeze-thaw effect forms ice crystals to block the flow  
59 path through large pores, subsequently limiting water infiltration (Stadler et al., 1997), while the melting  
60 effect of the infiltration water on ice makes it difficult to reach a steady infiltration state. Therefore, the  
61 current relevant achievements are mainly focused on the infiltration process of snowmelt water (Hayashi et  
62 al., 2003) and the influence of preferential flow (Mohammed et al., 2019). Controlled laboratory experiments  
63 provide new opportunities for the simulation of frozen soil infiltration ~~r~~ processes and the measurement of  
64 infiltration parameters. Williams and Burt (1974) conducted early direct measurements in the laboratory,  
65 resolved the water freezing problem by adding lactose and applied dialysis membranes on both sides of soil  
66 columns, and they determined the water conductivity of saturated specimens in the horizontal direction (Burt  
67 and Williams, 1976). Andersland et al. (1996) measured the hydraulic conductivity of frozen granular soils

68 at different saturations using a conventional drop permeameter with decane as the permeant and concluded  
69 that the hydraulic conductivity was the same as that of unfrozen soils with water as the infiltration solution.  
70 McCauley et al. (2002) determined and compared the differences in hydraulic conductivity, permeability and  
71 infiltration rate between frozen and unfrozen soils using diesel mixtures as permeants, and their results  
72 indicated that the ice content determines whether soil is sufficiently impermeable. Zhao et al. (2013)  
73 quantified the unsaturated hydraulic conductivity of frozen soil using antifreeze instead of water, adopted a  
74 multistage outflow method under controlled pressures and introduced the pore impedance coefficient.  
75 However, most of these studies did not consider the differences in kinematic viscosity and surface tension  
76 between soil water and other solutions, which often results in [an overestimation of hydraulic conductivity](#)  
77 ~~hydraulic conductivity estimation~~, and ~~the~~ homemade devices in the laboratory are often inconvenient for  
78 generalization in the field. Due to the dynamic changes in the temperature and moisture phase, direct  
79 measurement is difficult, and hydraulic conductivity empirical equations and models of frozen soil have been  
80 developed. First, the frozen soil hydraulic conductivity was simply considered to follow a power exponential  
81 relationship with the temperature (Nixon, 1991;Smith, 1985), while others considered the hydraulic  
82 conductivity of frozen soil to be equal to that of unfrozen soil at the same water content and assumed that  
83 the hydraulic conductivity of frozen soil was a function of the moisture content of unfrozen soil (Lundin,  
84 1990;Flerchinger and Saxton, 1989;Harlan, 1973). On the basis of Campbell's model (Campbell, 1985),  
85 Tarnawski and Wagner (1996) proposed a frozen soil hydraulic conductivity model based on the soil particle  
86 size distribution and porosity. Watanabe and Wake (2008) viewed soil pores as cylindrical capillaries and  
87 suggested that ice formation occurs at the center of these capillaries and established a model to describe the  
88 movement of thin film water and capillary water in frozen soil based on the theory of capillaries and surface  
89 absorption (Watanabe and Flury, 2008). The similarity between freezing and soil moisture profiles has been

90 demonstrated (Spaans and Baker, 1996; Spaans, 1994), and subsequently, ~~freezing profiles~~ [soil freezing](#)  
91 [characteristic curves](#) have been applied to estimate the unsaturated hydraulic conductivity of frozen soils  
92 (Azmatch et al., 2012), which has been combined with field tests and inversion models to achieve a high  
93 accuracy (Cheng et al., 2019).

94 Understanding the distribution characteristics of the soil pore system is essential for the evaluation of the  
95 water and heat movement processes in soil. ~~The soil~~ [Soil](#) macroporosity has been shown to impose a major  
96 impact on water cycle processes such as infiltration, nutrient movement and surface runoff. (Demand et al.,  
97 2019; Jarvis, 2007). ~~The macroporosity~~ [Macroporosity](#) is widespread in a variety of soils and produces  
98 preferential flow in both frozen and unfrozen soils (Mohammed et al., 2018; Beven and Germann, 2013), and  
99 the ~~pre~~-freeze moisture conditions affect the amount and state of ice in the macropores of frozen soils,  
100 resulting in a notable variability in the infiltration capacity of thawed soils (Hayashi et al., 2003; Granger et  
101 al., 1984). Field experiments on frozen soil have also demonstrated that macropores accelerate the infiltration  
102 rate (Stähli et al., 2004; Kamp et al., 2003), the number and size of macropores affect the freezing and  
103 infiltration capacity of soil layers to different extents, and low temperatures cause infiltration water to  
104 refreeze inside macropores (Watanabe and Kugisaki, 2017; Stadler et al., 2000). Research on ~~the~~ frozen soil  
105 macroporosity has largely focused on the qualitative analysis of its impact on the soil structure and  
106 infiltration capacity, and with the development of experimental techniques, certain new methods and  
107 techniques, such as computed tomography (CT) and X-ray scanning, have been applied to measure the  
108 number and distribution of macropores (Taina et al., 2013; Bodhinayake et al., 2004; Grevers et al., 1989),  
109 but the lack of sampling techniques targeting frozen soil still restricts related research.

110 Many limitations and deficiencies remain in the direct measurement of frozen soil infiltration characteristics  
111 and pore distribution, and the relevant models also require a large amount of measured data to meet the

112 accuracy and applicability requirements. In this paper, the stable infiltration rate and hydraulic conductivity  
 113 of three types of soils at different temperatures were measured by precise control of the soil and ambient  
 114 temperatures, and the macropore and mesopore size distribution was calculated by using a tension  
 115 infiltrometer and a glycol aqueous solution as the infiltration medium. The conclusions provide a basis and  
 116 reference for the numerical simulation of the coupled water-heat migration process of freezing-thawing soil  
 117 and related parameterization studies.

## 118 **2 Materials and methods**

### 119 **2.1 Test plan**

120 Referring to arable land area data of various regions of Heilongjiang Province, the three types of soils that  
 121 dominate the cultivated land area in ~~Heilongjiang~~ this province are black soils, ~~and~~ meadow soils and  
 122 chernozem (Bureau, 1992). Harbin, Zhaoyuan and Zhaozhou were selected as typical soil areas for sampling.  
 123 A 5-cm surface layer of floating soil and leaves was removed, and topsoil samples were collected at depths  
 124 ranging from 0-20 cm. After natural air drying and artificial crushing, the soil was sieved, and particles larger  
 125 than 2 mm in diameter were removed. The remainder was used to prepare soil columns. The basic physical  
 126 and chemical parameters of the test soils, such as the bulk density, organic content and mechanical  
 127 parameters, are listed in Table 1.

128 **Table 1**

129 **Basic physical and chemical properties of three kinds of soils**

Soil types	Bulk density (g/cm <sup>3</sup> )	Organic content (g/kg)	Electrical conductivity (s/m)	Particle size (sand- silt-clay) (%)	Soil texture
Black soil	1.31	28.32	0.02	12.64-70.82-16.54	silt loam

Meadow soil	1.22	16.51	0.01	9.52-73.00-17.48
Chernozem	1.15	26.52	0.01	38.99-50.30-10.71

130 An artificial climate chamber was applied to control the temperature of the soil column and infiltration  
131 solution, and four temperature treatments were established with three replications for each treatment: 15°C,  
132 unfrozen soil, representing the soil before freezing, which was recorded as 15°C (BF); -5°C, stable freezing;  
133 -10°C, stable freezing; and freezing at -10°C followed by thawing at 15°C, representing the soil after melting,  
134 which was recorded as 15°C (AM). [Each soil column was tested for only one treatment.](#) The freezing and  
135 thawing times were both 48 h. When the soil temperature was consistent with the set temperature in the  
136 climate chamber, the samples were considered to be completely frozen, and the effect of the number of  
137 freezing and thawing cycles was not considered in this test. According to the basic information of the original  
138 soil, the volumetric moisture content of the sieved soil was [set to 30% ± 2% using deionized water](#), with a  
139 dry bulk density of 1.2 g/cm<sup>3</sup>. [The soil porosity and pre-freezing soil water content of the repacked samples](#)  
140 [are shown in Table 2.](#)

141 **[Table 2](#)**

142 **[Soil porosity and pre-freezing soil water content of repacked samples](#)**

<a href="#">Soil types</a>	<a href="#">Soil porosity (%)</a>	<a href="#">Pre-freezing water content (%)</a>	
		<a href="#">-5°C</a>	<a href="#">-10°C</a>
<a href="#">Black soil</a>	<a href="#">52.76</a>	<a href="#">30.53</a>	<a href="#">29.27</a>
<a href="#">Meadow soil</a>	<a href="#">52.82</a>	<a href="#">29.83</a>	<a href="#">30.70</a>
<a href="#">Chernozem</a>	<a href="#">53.22</a>	<a href="#">30.07</a>	<a href="#">30.93</a>

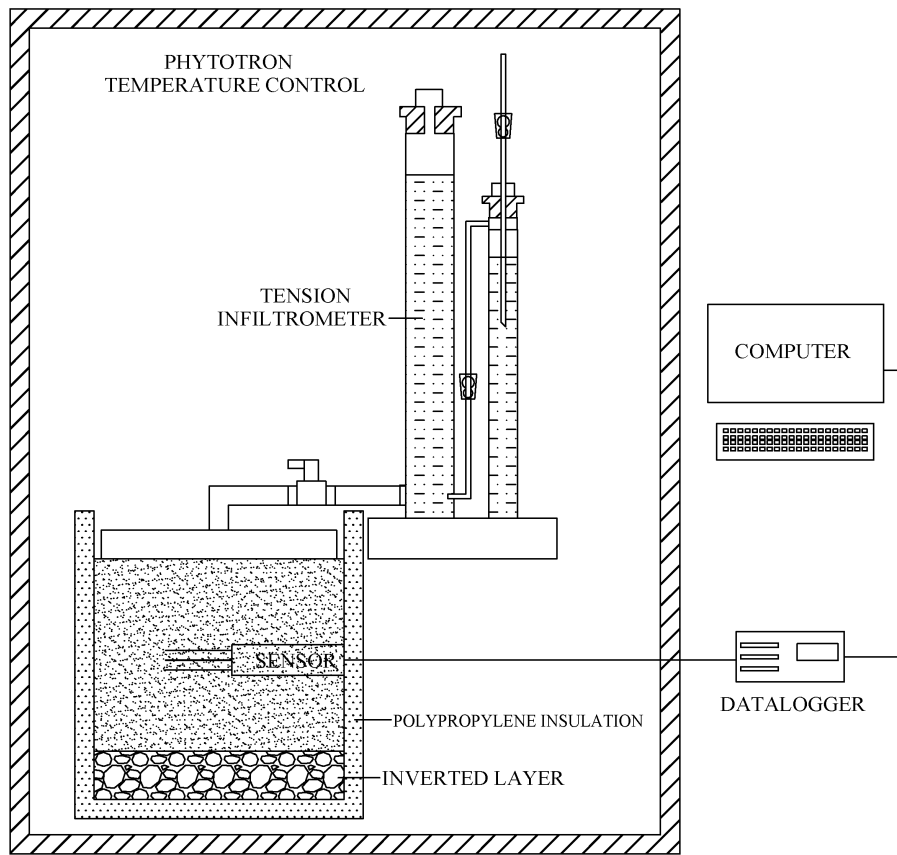
143 To ensure a homogeneous column, the soil was loaded into a polyvinyl chloride (PVC) cylinder at 5-cm  
144 depth intervals, and petroleum jelly was applied to the sides to reduce the sidewall flow (Lewis and Sjöström,  
145 2010). The PVC cylinder was 26 cm in diameter and 30 cm in height, with a perforated plate at the bottom.

146 To prevent lateral seepage, the barrel occurred 5 cm above the soil surface, and the thickness of the soil layer  
147 was 20 cm. A HYDRA-PROBE II sensor (STEVENS Water Monitoring Systems, Inc., Portland, Oregon,  
148 USA) was inserted in the middle of the ~~pail~~-barrel to observe the potential soil temperature and liquid water  
149 content change to determine whether ice melting occurred. and the ice content of frozen soil was measured  
150 by the drying method. A 5-cm thick layer of sand and gravel was ~~em~~placed below the soil column, and a 5-  
151 cm thick layer of black polypropylene insulation cotton was wrapped around the outer layer and the bottom  
152 of the soil column. The stable infiltration rate under tension levels of -3, -5, -7, -9, -11, and -13 cm was  
153 measured with a tension infiltrometer, and the infiltration time and cumulative infiltration were recorded.  
154 The detailed layout of the test apparatus is shown in Fig. 1.

155 The addition of a certain amount of lactose, antifreeze or other substances to water greatly reduces the  
156 freezing point of water (Zhao et al., 2013; Williams and Burt, 1974) so that the soil macropores are not  
157 quickly filled with ice with decreasing temperature, thereby maintaining better conditions for water flow. To  
158 further verify the feasibility of the use of deionized water to prepare an aqueous solution of ethylene glycol  
159 at a mass concentration of 40% as the infiltration medium for the frozen soil measurements, the surface  
160 tension of the aqueous glycol solution at -5°C and -10°C and its relationship with the temperature were  
161 measured with a contact angle measuring instrument (OCA20, DataPhysics Instruments, Germany) and a  
162 surface tension measuring instrument (DCAT-21, DataPhysics Instruments, Germany), respectively. As an  
163 example, the contact angle measurement process of the black soil at -10°C with the aqueous ethylene glycol  
164 solution is shown in Fig. 2, and it is observed that the contact angle decreases to 0° within a few seconds  
165 after the liquid droplet is placed on the soil, and the liquid droplet completely dissolves in the frozen soil,  
166 which implies that the addition of glycol to water does not alter the wetting ability of the soil particles (Lu  
167 and Likos, 2004). The relevant physicochemical properties of the aqueous ethylene glycol solution and water



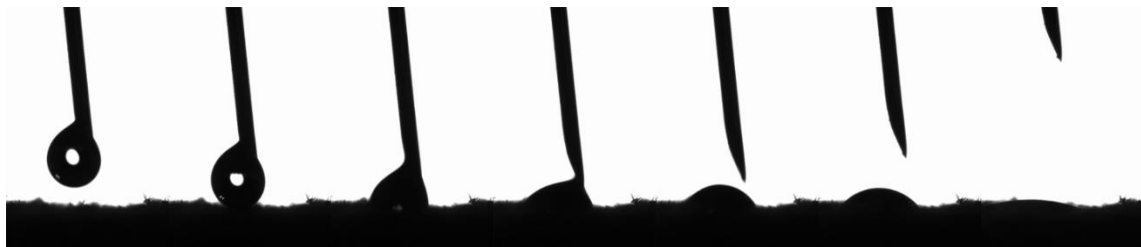
168 are compared in Table 23.



169

170

Fig. 1. Diagram of the test equipment.



171

172 Fig. 2. Process of the contact angle measurement between the aqueous ethylene glycol solution and black

173

soil at -10°C.

174 Table 23

175 Comparison of the physicochemical properties of the 40% ethylene glycol aqueous solution and

176 water

---

Infiltration solution	Temperature	Density	Dynamic	Surface tension	Contact
-----------------------	-------------	---------	---------	-----------------	---------

---

	(°C)	(g/cm <sup>3</sup> )	viscosity (mPa.s)	(mN/m)	angle (°)
Water	15	0.9991	1.14	73.56	0
Ethylene glycol	-5	1.0683	7.18	48.89	0
aqueous solution	-10	1.0696	9.06	49.10	0

## 177 2.2 Measurement of the frozen soil hydraulic conductivity

178 Gardner (1958) proposed that the unsaturated hydraulic conductivity of soil varies with the matric potential

179 [as follows:](#)

$$180 \quad K(h) = K_{sat} \exp(\alpha h) \quad (1)$$

181 where  $K_{sat}$  is the saturated hydraulic conductivity, cm/hour, and  $h$  is the matric potential or tension, cm H<sub>2</sub>O.

182 Wooding (1968) considered that the steady-state unconfined infiltration rate into soil from a circular water

183 source of radius  $R$  can be calculated with the following equation:

$$184 \quad Q = \pi R^2 K \left[ 1 + \frac{4}{\pi R \alpha} \right] \quad (2)$$

185 where  $Q$  is the amount of water entering the soil per unit time, cm<sup>3</sup>/h;  $K$  is the hydraulic conductivity,

186 cm/hour; and  $\alpha$  is a constant. Ankeny et al. (1991) proposed that implementing two successively applied

187 pressure heads  $h_1$  and  $h_2$  could yield the unsaturated hydraulic conductivity, and upon replacing  $K$  in Eq. (2)

188 with Eq. (1), the following is obtained:

$$189 \quad Q(h_1) = \pi R^2 K_{sat} \exp(\alpha h_1) \left[ 1 + \frac{4}{\pi R \alpha} \right] \quad (3)$$

$$190 \quad Q(h_2) = \pi R^2 K_{sat} \exp(\alpha h_2) \left[ 1 + \frac{4}{\pi R \alpha} \right] \quad (4)$$

191 Dividing Eq. (4) by Eq. (3) and solving for  $\alpha$  yields:

$$192 \quad \alpha = \frac{\ln[Q(h_2) / Q(h_1)]}{h_2 - h_1} \quad (5)$$

193 where  $Q(h_1)$  and  $Q(h_2)$  can be measured,  $h_1$  and  $h_2$  are the preset tension values, and  $\alpha$  can be calculated with  
194 Eq. (5). The result can be substituted into Eq. (3) or (4) to calculate  $K_{sat}$ . When the number of tension levels  
195 is ~~larger~~ higher than 2, parameter fitting methods can be applied to improve the accuracy of  $\alpha$  and  $K_{sat}$   
196 (Hussen and Warrick, 1993).

197 The tension is controlled by the bubble collecting tube of the tension infiltrometer, and different pressure  
198 heads  $h$  correspond to different pore sizes  $r$ . By applying different pressure heads  $h$  to the soil surface, water  
199 will overcome the surface tension in the corresponding pores and will be discharged, and the infiltration  
200 volume is recorded after reaching the stable infiltration state.

201 Under the assumption that the frozen soil pore ice pressure is equal to the atmospheric pressure and that  
202 solutes are negligible, the Clausius-Clapeyron equation can be adopted to achieve the interconversion  
203 between the soil temperature and suction (Konrad and Morgenstern, 1980; Watanabe et al., 2013), which can  
204 be simplified as follows:

$$205 \quad \psi = -L\rho_w \frac{T}{273.15} \quad (6)$$

206 where  $\psi$  is the soil suction, kPa;  $L$  is the latent heat of fusion of water,  $3.34 \times 10^5$  J/kg;  $\rho_w$  is the density of  
207 water,  $1 \text{ g/cm}^3$ ; and  $T$  is the subfreezing temperature, °C. After the unit conversion of the soil suction into  $h$   
208 (cm  $\text{H}_2\text{O}$ ), the unsaturated hydraulic conductivity of frozen soil at different negative temperatures can be  
209 obtained via substitution into Eq. (2).

### 210 **2.3 Measurement of the pore size distribution in frozen soil**

211 As a nonuniform medium, soil consists of pores ~~of~~ with various pore sizes, and the equation for the soil pore  
212 radius  $r$  can be obtained from the capillary model (Watson and Luxmoore, 1986):

$$213 \quad r = -\frac{2\sigma \cos \beta}{\rho gh} \quad (7)$$

214 where  $\sigma$  is the surface tension of the solution, g/s<sup>2</sup>;  $\beta$  is the contact angle between the solution and pore wall;  
215  $\rho$  is the density of the solution, g/cm<sup>3</sup>;  $g$  is the acceleration of gravity, m/s<sup>2</sup>; and  $h$  is the corresponding tension  
216 of the tension infiltrometer, cm H<sub>2</sub>O.

217 The effective macroporosity  $\theta_m$  can be calculated for various soil particle sizes based on the Poiseuille  
218 equation (Wilson and Luxmoore, 1988):

$$219 \quad \theta_m = 8\mu K_m / \rho g r^2 \quad (8)$$

220 where  $\mu$  is the dynamic viscosity of the fluid, g/(cm\*s);  $K_m$  is the macropore hydraulic conductivity and is  
221 defined as the difference between  $K(h)$  at various tension gradients, cm/h; and  $r$  is the corresponding  
222 equivalent pore size. The effective porosity is equal to the number of pores per unit area multiplied by the  
223 area of the corresponding pore size. For different pore sizes, the maximum number of effective macropores  
224 per unit area  $N$  can be calculated with the following equation:

$$225 \quad N = \theta_m / \pi r^2 \quad (9)$$

226 where  $N$  is the number of effective macropores per unit area, and Eq. (7) calculates the minimum value of  
227 the pore radius, while the result obtained with Eq. (9) is actually the maximum number of effective  
228 macropores per unit area and the maximum porosity.

229 Considering the differences in surface tension and density between the aqueous ethylene glycol solution and  
230 water, when calculating the frozen soil pore size distribution, it is necessary to convert the tension into the  
231 equivalent pore radius according to Eq. (7), which is classified and subdivided into large and medium pores  
232 according to the common classification method (Luxmoore, 1981), the details of which are listed in Table  
233 [3-4](#), while the corresponding tension values in Table [3-4](#) are substituted into the fitting curve equation to  
234 calculate the corresponding stable infiltration rate  $q$  and unsaturated hydraulic conductivity  $K$ .

235 **Table [3-4](#)**

236 **Tension and equivalent pore radius conversions**

Pore types	Pore radius (mm)	Tension conversion (cm)		
		Water (15°C)	Ethylene glycol aqueous solution (- 5°C)	Ethylene glycol aqueous solution (- 10°C)
Macroporous	>0.5	0~3	0~1.86	0~1.87
	0.3-0.5	3~5	1.86~3.11	1.86~3.12
Mesoporous	0.15-0.3	5~10	3.11~6.22	3.12~6.23
	0.1-0.15	10~15	6.22~9.32	6.23~9.35
	0.05-0.1	15~30	9.32~18.65	9.35~18.70

237 **3 Results**

238 **3.1 Infiltration characteristics of freezing-thawing soils**

239 ~~According to the recorded cumulative infiltration and duration, e~~Curves of the recorded cumulative  
 240 infiltration and infiltration rate were plotted over time, as shown in Figs. 3 and 4, respectively. The unfrozen  
 241 water contents and ice contents of the frozen samples are shown in Table 5. The constant  $\alpha$  and saturated  
 242 hydraulic conductivity  $K_{sat}$  were calculated under different tensions  $h$  and corresponding steady-state  
 243 infiltration rates  $q$ , and the unsaturated hydraulic conductivity under different tensions was calculated with  
 244 Eq. (1). The stable infiltration rate and unsaturated hydraulic conductivity at different temperatures are  
 245 shown in Fig. 5, and the details of  $\alpha$  and  $K_{sat}$  are listed in Table 46.

246 **Table 5**

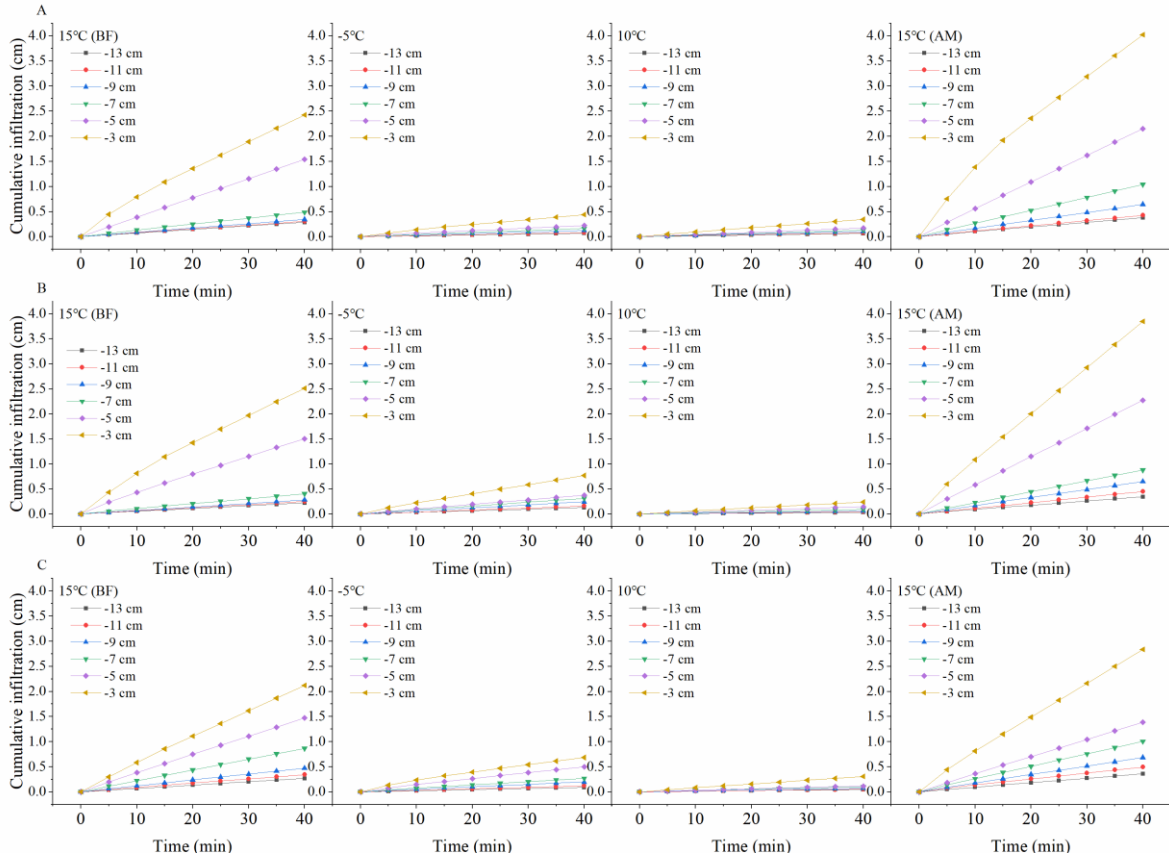
247 **Unfrozen water contents and ice contents of the frozen samples**

Soil types	Unfrozen water contents (cm <sup>3</sup> /cm <sup>3</sup> )		Ice contents (cm <sup>3</sup> /cm <sup>3</sup> )	
	<u>-5°C</u>	<u>-10°C</u>	<u>-5°C</u>	<u>-10°C</u>

<u>Black soil</u>	<u>0.123</u>	<u>0.101</u>	<u>0.159</u>	<u>0.179</u>
<u>Meadow soil</u>	<u>0.128</u>	<u>0.109</u>	<u>0.145</u>	<u>0.167</u>
<u>Chernozem</u>	<u>0.119</u>	<u>0.097</u>	<u>0.151</u>	<u>0.185</u>

248

249

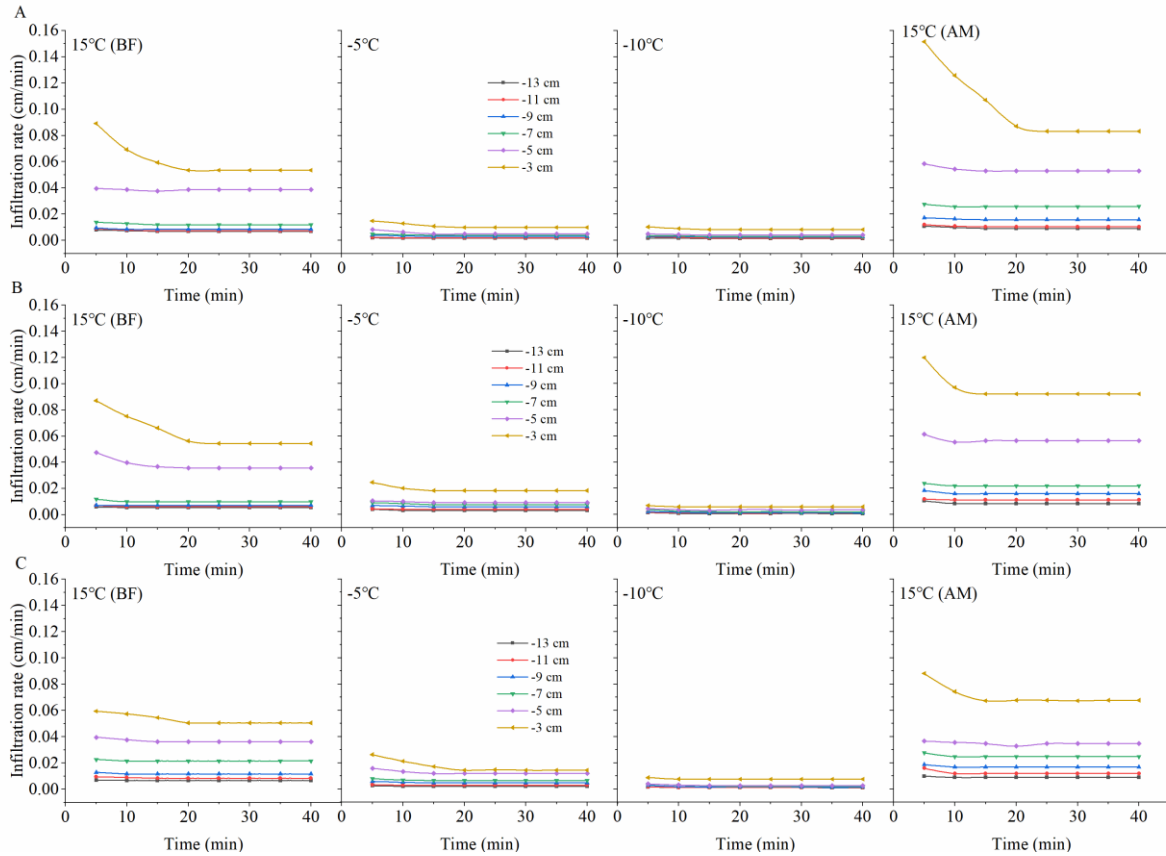


250

251 **Fig. 3.** Cumulative infiltration over time under the different treatments.

252 Note: A Black Soil; B Meadow Soil; C Chernozem.

253



254

255 **Fig. 4.** Infiltration rate over time under the different treatments.

256 Note: A Black Soil; B Meadow Soil; C Chernozem.

257 As shown in Figs. 4 and 5, under the different tension conditions, the infiltration capacity of the unfrozen

258 soil is basically consistent with the findings of field experiments and is highly influenced by the tension

259 value (Wang et al., 1998). Compared to the room-temperature soil, the cumulative infiltration of frozen soil

260 slowly increases, and the infiltration rate always remains low, while under the same negative temperature

261 treatment, the influence of the tension value is also greatly reduced. When the temperature was reduced to -

262 10°C, few major tension differences were observed except for the maximum tension of -3 cm. ~~From~~ Based

263 on the change in the slope of the two curves, ~~we find that~~ the time for the unfrozen soil to reach the stable

264 infiltration rate usually ranged ~~s~~ from 15~20 min, while the time for the frozen soil to reach the stable

265 infiltration rate ~~is~~ was usually 10 min under higher tensions of -3 and -5 cm and 5 min under lower tensions.

266 ~~Comparing~~ A comparison of the infiltration process before and after the freezing and thawing of the soil

267 [indicated that](#); overall, the cumulative infiltration and infiltration rate exhibited varying degrees of increase  
 268 with increasing tension value, and the increase amplitude expanded. Moreover, the difference in the  
 269 cumulative infiltration and infiltration rate between the low tension levels ranging from -9 to -13 cm after  
 270 soil thawing was larger than that before soil freezing, which also indirectly demonstrated that freezing and  
 271 thawing could further stabilize the soil pore distribution by affecting the homogeneity, which will be detailed  
 272 in subsequent sections.

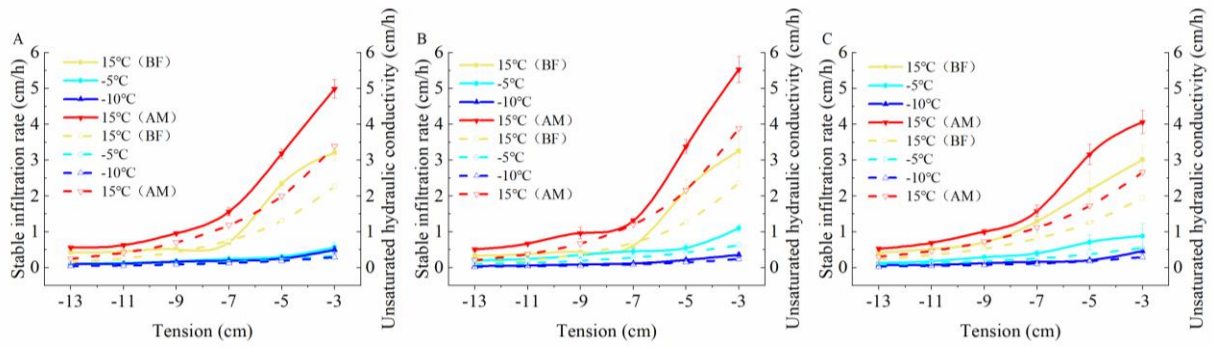
273 **Table 46**

274 **Infiltration parameters of the different temperature treatments of the three soil types**

Soil types	Temperature (°C)	$\alpha$ (cm/h)	$K_{sat}$ (cm/h)
Black soil	15 (BF)	0.2742	5.1480
	-5	0.1993	0.5960
	-10	0.2028	0.5221
	15 (AM)	0.2629	7.4658
Meadow soil	15 (BF)	0.3071	5.9232
	-5	0.1996	1.1385
	-10	0.2477	0.4903
	15 (AM)	0.2934	9.3757
Chernozem	15 (BF)	0.2166	3.7185
	-5	0.1907	0.9739
	-10	0.2508	0.6077
	15 (AM)	0.2182	5.1283

275





276

277

**Fig. 5.** Variation curves of the unsaturated hydraulic conductivity and stable infiltration rate with the

278

tension for the different treatments of the three soils.

279

Note: A Black soil; B meadow soil; C chernozem. The solid lines represent the stable infiltration rate, and

280

the dashed lines represent the unsaturated hydraulic conductivity.

281

~~Combining~~ By combining Fig. 5 and Table-4\_6, we observe that the three types of soils exhibit a high

282

infiltration capacity under normal temperature conditions. With increasing set tension value, the suction force

283

of the soil matrix gradually ~~weakens~~ weakened, the constraint and maintenance capacity of the matric

284

potential with respect to the soil water ~~decreases~~ decreased, the number of pores involved in the soil water

285

infiltration process increases, and the unsaturated hydraulic conductivity and stable infiltration rate of the

286

three types of soils ~~all reveal~~ exhibited different degrees of increase. When the temperature was lowered from

287

15°C to -5°C and the soil reached the stable frozen state, the saturated water conductivity of the black soil,

288

meadow soil and chernozem soil decreased by 88.42%, 80.78% and 73.8%, respectively. ~~With~~ When the

289

~~decreasing~~ soil temperature was decreased to -10 °C, due to the presence of liquid water in the pores, the

290

saturated water conductivity still exhibited a certain decrease over the pre-freeze conditions and continued

291

to decrease by 1.43%, 10.94% and 9.85%, respectively. At negative temperatures, the unsaturated hydraulic

292

conductivity decreased considerably and fluctuated within a small range, mainly because the unfrozen water

293

content and saturated ~~water contents~~ hydraulic conductivity were low after soil freezing. ~~Comparing~~ Based

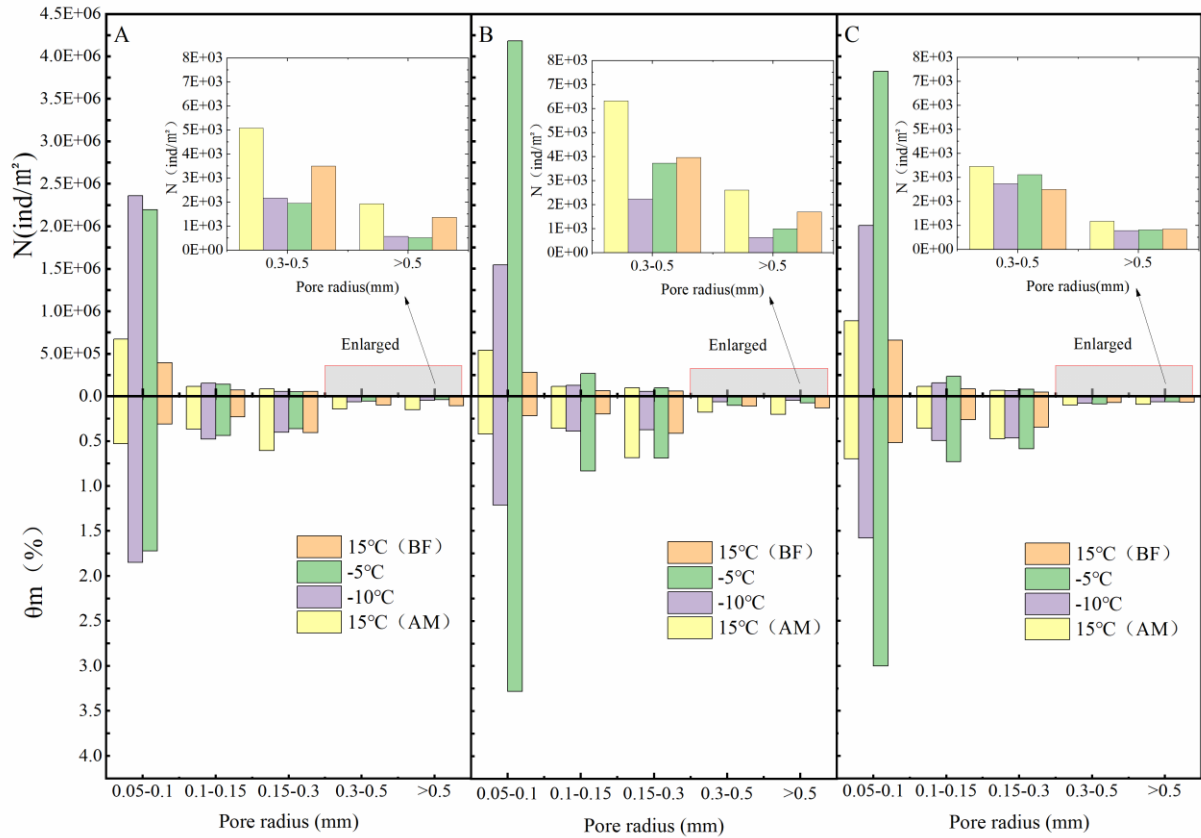
294

on a comparing of the ~~two treatments of~~ -5°C and -10°C treatments, the unsaturated hydraulic conductivity

295 (ANOVA, P=0.72, F=0.14) and stable infiltration rate (ANOVA, P=0.71, F=0.15) of the black soil ~~revealed~~  
296 exhibited almost no significant change, indicating that most of its pores were filled with ice crystals at -5°C  
297 and were no longer involved in water infiltration. The unsaturated water conductivity of the meadow and  
298 chernozem soils still exhibited a more significant reduction when the freezing temperature was further  
299 reduced to -10°C. When the temperature was raised again to 15°C and the soil was completely thawed, the  
300 steady infiltration rate and saturated hydraulic conductivity increased with increasing temperature, and the  
301 values were higher than those of the soil at the same temperature before freezing. The saturated hydraulic  
302 conductivity of the black soil, meadow soil and chernozem increased by 45.02%, 58.63% and 37.91%,  
303 respectively, ~~over~~ relative to the 15°C (BF) treatment values.

### 304 **3.2 Pore distribution characteristics of the freezing-thawing soil**

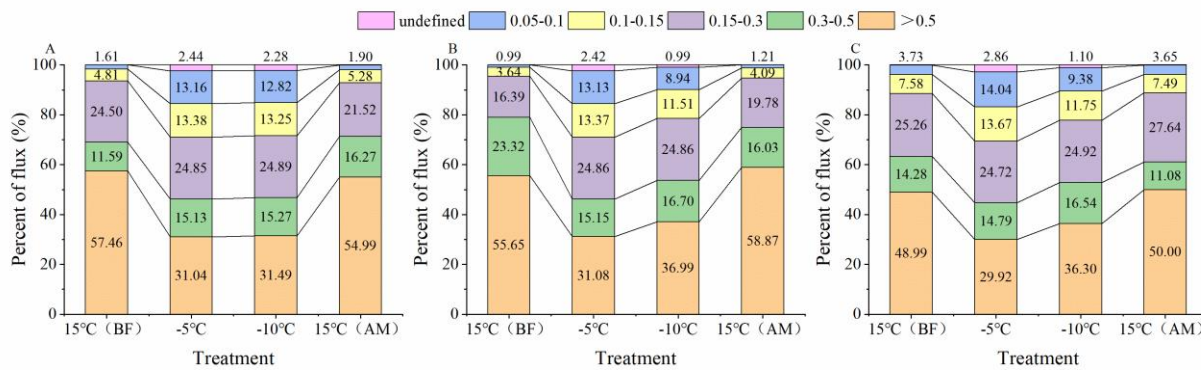
305 Considering the differences in the physical and chemical properties between the infiltration solutions,  
306 infiltration parameters such as the hydraulic conductivity and stable infiltration rate alone do not fully reflect  
307 the infiltration characteristics and internal pore size of frozen soils. According to Eqs. (7)-(9), the maximum  
308 number per unit area  $N$ , effective porosity  $\theta_m$  and percentage of pore flow to saturated flow  $P$  corresponding  
309 to the different soil pore sizes of the three soils under the different temperature treatments ~~are~~ were calculated,  
310 as shown in Figs. 6 and 7.



311

312 **Fig. 6.** Number of pores and effective porosity of the different equivalent pores.

313 Note: A Black Soil; B Meadow Soil; C Chernozem.



314

315 **Fig. 7.** Percentage of the pore flow in the saturated flow for the different equivalent pore sizes.

316 Note: A Black Soil; B Meadow Soil; C Chernozem.

317 Fig. 6 shows that pores of different equivalent radii widely occur in all three soils, and under all four  
 318 temperature treatments, the largest N value is that for the medium pores with an equivalent radius of 0.05-  
 319 0.1 mm, and N gradually decreases with increasing equivalent radius size. Under the two room-temperature

320 treatments at 15°C (BF) and 15°C (AM), the largest number of 0.05- to 0.1-mm medium pores and the  
321 smallest number of >0.5-mm macropores differed by two orders of magnitude, and the number of pores of  
322 each size exhibited different degrees of increase or decrease ~~over~~-in the two treatments at -5°C and -10°C  
323 where freezing occurred, with the number of medium pores with an equivalent pore size of 0.05-0.1 mm  
324 significantly changing. Increases of more than an order of magnitude were achieved in all three soils, while  
325 the macropores with an equivalent pore size of >0.5 mm were generally reduced by an order of magnitude,  
326 with the difference in the number of pores of these two sizes reaching four orders of magnitude. This  
327 indicates that freezing caused by temperature change significantly alters the soil internal structure, with ice  
328 crystals forming in the relatively large pores containing the internal soil moisture, resulting in a large number  
329 of smaller pores. Based on an assessment of ~~Assessing~~ the two treatments at -5°C and -10°C separately, when  
330 the temperature was lowered from -5°C to -10°C, the number of pores in each pore size interval of the  
331 meadow and chernozem soils exhibited a significant decrease, while the black soil revealed a small increase,  
332 which might be related to the high organic matter content of the black soil. A comparison of ~~Comparing~~ the  
333 two treatments at 15°C (BF) and 15°C (AM) indicated that, the number of pores in all three soils increased  
334 to different degrees after thawing, and more pores were formed with the melting of ice crystals after the  
335 freeze-thaw destruction of the soil particles, which enhanced the soil water conductivity.

336 Comprehensive analysis of Figs. 6 and 7 reveals that before freezing, the  $\theta_m$  values of the various pore sizes  
337 of the black soils, ~~and~~ meadow soils and chernozem with an equivalent radius of >0.5 mm were 0.11%, 0.13%  
338 and 0.07%, respectively, while the P value reached 57.46%, 55.65% and 48.99%, respectively, with the  
339 values of the thawed soil similar to these values. This indicates that for all five soil pore sizes under unfrozen  
340 conditions, although the number of macropores with a pore size >0.5 mm was ~~is~~ the smallest and the effective  
341 porosity was ~~is~~ the lowest, their contribution to the saturated flow was ~~is~~ usually more than half, and the

342 macropores needed ~~to only~~ represent only a small fraction of the pore volume to significantly contribute to  
343 the soil water flow. For the frozen soil, the P value of the >0.5-mm macropores was significantly reduced  
344 and remained at approximately 30% after the reduction, while the P value of the smaller pore sizes such as  
345 0.15-0.3 mm, 0.1-0.15 mm, and 0.05-0.1 mm, revealed different degrees of increase. Moreover, the smaller  
346 the pore size ~~was~~, the greater the P value increased, and ~~their~~ the contribution of these pores eventually  
347 accounted for more than 10% of the saturated flow. The saturated flow became more evenly distributed  
348 across the pores of each size, and the total proportion of medium pores exceeded that of the macropores.  
349 This indicates that the freezing action caused obvious changes to the soil structure, pore size and quantity,  
350 and although the macropores still played an important role, the infiltration capacity of the frozen soil no  
351 longer relied solely on these macropores, and the contribution of certain smaller-sized mesopores to the  
352 infiltration capacity of the frozen soil could no longer be neglected. Selecting ~~the~~ black soil as an example,  
353 the total effective porosity of the pores of each size under the four treatments was 1.15%, 2.62%, 2.84%, and  
354 1.80%, and the P values were 99.97%, 97.56%, 97.72%, and 99.96%, respectively, which implies that the  
355 soil water infiltrated almost entirely via the large and medium pores. The small micropores, even in large  
356 numbers, contributed little to the infiltration process.

## 357 **4 Discussion**

### 358 **4.1 Permeability and hydraulic conductivity of the frozen soil**

359 It is worth noting that the theory underpinning the tension infiltration analysis in this article is based on the  
360 assumption that larger pores only flow fully saturated which means no air-water interface inside the pore and  
361 excludes the formation of an air-water interface with flowing water in larger pores (Perroux and White, 1988).  
362 However, recent work has shown that this flow mode does indeed occur (Beven and Germann, 2013; Nimmo,  
363 2012, 2010).

364 In the field environment, although it is difficult to accurately measure the infiltration rate of frozen soils  
365 using traditional instruments and methods such as single-loop infiltrators, the obtained test results still  
366 demonstrate that the infiltration capacity decreases by one or more orders of magnitude when the soil is  
367 frozen (Stähli et al., 2004). Although the cumulative infiltration and infiltration rate of frozen soil are low,  
368 the presence of unfrozen water allows a certain amount of infiltration flow to be maintained in the soil. When  
369 water is applied as the infiltration solution, the low temperature ~~in~~-of the frozen soil easily causes the  
370 infiltration water to freeze, thus forming a thin layer of ice on the soil particle surface and delaying the  
371 subsequent infiltration of water. This phenomenon results in a low infiltration rate after the freezing of soils  
372 with a high initial water content and a relatively high infiltration rate after the freezing of dry soils (Watanabe  
373 et al., 2013), because the higher the ice content is, the more latent heat needs to be overcome to melt any ice  
374 crystals, resulting in a weakened propagation of the melting front, thus limiting the infiltration rate so that it  
375 is controlled by the downward movement of the melting leading edge of the ice crystals (Pittman et al., 2020).  
376 During the measurements using the tension infiltrator in this study, the sensor temperature always remained  
377 consistent with the soil temperature, indicating that the use of an aqueous glycol solution could be a useful  
378 way to avoid the problem of freezing of the infiltration solution. In addition, the hydraulic conductivity of  
379 frozen soils with different capacities and at various water flow rates was demonstrated not to greatly differ  
380 (Watanabe and Osada, 2017).  
381 Whether water or other low-freezing point solutions are applied as infiltration media, the hydraulic  
382 conductivity of frozen soil significantly changes only within a limited temperature range above  $-0.5^{\circ}\text{C}$   
383 depending on the unfrozen water and ice contents, and at a soil temperature below  $-0.5^{\circ}\text{C}$ , the hydraulic  
384 conductivity usually decreases to ~~below~~-less than  $10^{-10}$  m/s (Watanabe and Osada, 2017; Williams and Burt,  
385 1974). The unsaturated hydraulic conductivity in our experiments was measured at a set tension level, and

386 according to Eq. (6), the soil substrate potential increases by 125 m for every 1°C decrease in temperature  
387 (Williams and Smith, 1989), while the frozen soil hydraulic conductivity calculated at -5°C and -10°C, which  
388 corresponds to the actual matric potential, is much lower than  $10^{-10}$  m/s and can be ignored. This suggests  
389 that even under ideal conditions where no heat exchange occurs between the infiltration solution and the soil  
390 and no freezing of the infiltration water takes place to prevent ~~the~~ subsequent infiltration, the unsaturated  
391 hydraulic conductivity of ~~the~~ frozen soil is so low that the frozen soil at lower temperatures in its natural  
392 state could be considered impermeable, ~~both with respect to both for~~ water and other solutions.

#### 393 4.2 Effect of ~~the~~ freeze-thaw cycles on soil pore distribution

394 In our study, the N value after freezing for the different types of soil was approximately 1000-2000/m<sup>2</sup> ~~base~~  
395 ~~on using~~ the tension infiltrator, which agreed well with other studies and remained at a same magnitude  
396 (Pittman et al., 2020), indicating that the method is generally reliable. The freeze-thaw effect significantly  
397 improves the water conductivity of the different types of soils because it increases the porosity, decreases  
398 the soil compactness and dry weight, and thus increases the soil water conductivity (Fouli et al., 2013). On  
399 this basis, we also found that the freeze/thaw process significantly ~~alters~~ ~~altered~~ the size and number of soil  
400 pores, especially after freezing, and the number of macropores ~~decreases~~ ~~decreased~~, while the contribution  
401 of macropores to the saturated flow ~~decreases~~ ~~decreased~~. The proportion of the saturated flow in the  
402 mesopores with a pore size of <0.3 mm ~~approaches~~ ~~approached~~ or even ~~exceeds~~ ~~exceeded~~ the proportion in  
403 the macropores, indicating that the soil water inside relatively large pores is more likely to freeze, which in  
404 turn creates a large number of small pores, whereas the water transfer process in unfrozen soils primarily  
405 relies on the macropores, with obvious differences (Wilson and Luxmoore, 1988; Watson and Luxmoore,  
406 1986). The unsaturated water conductivity of the frozen soils measured in this study ~~is~~ ~~was~~ quite low, but  
407 under human control (Watanabe and Kugisaki, 2017) or natural conditions in the field (Espeby, 1990), water

408 has been shown to infiltrate ~~into~~-frozen soils through macropores as long as the pore size is large enough.

409 Considering that the soil in this experiment ~~is~~-was disturbed soil that ~~has~~-had been air dried and sieved,

410 although the macropores created by tillage practices (Lipiec et al., 2006) and invertebrate activities (Lavelle

411 et al., 2006) ~~are~~-were excluded, due to the inherent heterogeneity of the soil particles, macropores remain in

412 the uniformly filled soil column (Cortis and Berkowitz, 2004;Oswald et al., 1997), and these macroporous

413 pores still played a role in determining the infiltration water flow.

414 ~~Studies~~-There are still only a few studies related to ~~the~~-frozen soil macropore flow and pore distribution;

415 consequently~~are still quite few and~~, more data should be acquired and more models should be developed to

416 better understand ~~the~~-water movement in frozen soil regions. The experiments in this paper are based on

417 repacked soils that were subjected to the first freeze-thaw cycle in the laboratory, and the conclusions may

418 not be comprehensive. ~~in~~-In subsequent studies, we will consider applying the methods used in this paper to

419 field experiments to examine the dynamics of the infiltration capacity and pore distribution in

420 nonhomogeneous soils during whole freeze-thaw periods under real outdoor climatic conditions, such as

421 lower temperatures and more severe freeze-thaw cycles, but the infiltration solution must be carefully

422 selected; as ethylene glycol has low toxicity~~is toxic~~, to prevent contamination of agricultural soils and crops,

423 ~~and~~-a certain concentration of lactose could be considered (Burt and Williams, 1976;Williams and Burt,

424 1974). At room temperature, an ethylene glycol aqueous solution and water have similar densities and

425 relatively similar viscosities. We have compared these two infiltration solutions in unfrozen soil field

426 experiments, and the infiltration and pore conditions were basically similar, so we still used an aqueous

427 glycol solution in the frozen soil laboratory experiment. Measurements should focus on frozen soil layers at

428 different depths, especially in the vicinity of freezing peaks, and the spatial variability in the distribution of

429 frozen soil pores should be investigated. This work helps to improve the accuracy of simulations such as



430 those of frozen soil water and heat movement or snowmelt water infiltration processes.

## 431 **5 Conclusions**

432 In this paper, the infiltration capacity of soil columns under four temperature treatments representing various  
433 freeze-thaw stages was measured, and the distribution of the pores of various sizes within the soil was  
434 calculated based on the measurements by applying an aqueous ethylene glycol solution with a tension  
435 infiltrator in the laboratory. The results revealed that for the three types of soils, i.e., black soil, meadow soil  
436 and chernozem, the macropores, which accounted for only approximately 0.1% to 0.2% of the soil volume  
437 at room temperature, contributed approximately 50% to the saturated flow, and after freezing, the proportion  
438 of macropores decreased to 0.05% to 0.1%, while their share of the saturated flow decreased to  
439 approximately 30%. Coupled with the even smaller mesopores, the large and medium pores, accounting for  
440 approximately 1% to 2% of the soil volume, conducted almost all of the soil moisture under saturated  
441 conditions. Freezing decreased the number of macropores and increased the number of smaller-sized  
442 mesopores, thereby significantly increasing their contribution to the frozen soil infiltration capacity so that  
443 the latter was no longer solely dependent on the macropores. The infiltration parameters and pore distribution  
444 of the black soil were the least affected by the different negative freezing temperatures under the same  
445 moisture content and weight capacity conditions, while those of the meadow soil were the most impacted.

## 446 **Data availability**

447 Data used in this study are available ~~in the~~at Figshare (doi: [10.6084/m9.figshare.12965123](https://doi.org/10.6084/m9.figshare.12965123)-).

## 448 **Author contributions**

449 Ruiqi Jiang designed [the](#) research program. Tianxiao Li and Ruiqi Jiang built and deployed the soil column  
450 and instruments with assistance from Qinglin Li and Renjie Hou. Dong Liu and Qiang Fu provided funding  
451 for test equipment. Song Cui collected soil samples in the field. Ruiqi Jiang and Tianxiao Li analyzed the

452 laboratory data. Ruiqi Jiang prepared the manuscript with comments from Tianxiao Li and Dong Liu.

### 453 **Competing interests**

454 The authors declare that they have no conflicts of interest

### 455 **Acknowledgements**

456 We acknowledge that this research was supported by the National Natural Science Foundation of China  
457 (51679039), the National Science Fund for Distinguished Young Scholars (51825901), the Heilongjiang  
458 Provincial Science Fund for Distinguished Young Scholars (YQ2020E002),"Young Talents" Project of  
459 Northeast Agricultural University(18QC28), [and the](#) China Postdoctoral Science Foundation Grant  
460 (2019M651247).

### 461 **References**

462 Andersland, O. B., Wiggert, D. C., and Davies, S. H.: Hydraulic conductivity of frozen granular soils, *J*  
463 *Environ Eng*, 122, 212-216, 10.1061/(ASCE)0733-9372(1996)122:3(212), 1996.

464 Angulo-Jaramillo, R., Vandervaere, J.-P., Roulier, S., Thony, J.-L., Gaudet, J.-P., and Vauclin, M.: Field  
465 measurement of soil surface hydraulic properties by disc and ring infiltrometers: A review and recent  
466 developments, *Soil and Tillage Research*, 55, 1-29, 10.1016/S0167-1987(00)00098-2, 2000.

467 Ankeny, M. D., Ahmed, M., Kaspar, T. C., and Horton, R.: Simple field method for determining  
468 unsaturated hydraulic conductivity, *Soil Sci Soc Am J*, 55, 467-470,  
469 10.2136/sssaj1991.03615995005500020028x, 1991.

470 Azmatch, T. F., Segó, D. C., Arenson, L. U., and Biggar, K. W.: Using soil freezing characteristic curve to  
471 estimate the hydraulic conductivity function of partially frozen soils, *Cold Reg. Sci. Technol*, 83, 103-109,  
472 10.1016/j.coldregions.2012.07.002, 2012.

473 Beven, K., and Germann, P.: Macropores and water flow in soils revisited, *Water Resour Res*, 49, 3071-

474 3092, 10.1002/wrcr.20156, 2013.

475 Bodhinayake, W., Si, B. C., and Xiao, C.: New method for determining water - conducting macro - and  
476 mesoporosity from tension infiltrometer, *Soil Sci Soc Am J*, 68, 760-769, 10.2136/sssaj2004.0760, 2004.

477 Bureau, H. L. A.: Heilongjiang soil, Agriculture Press, Beijing, 1992.

478 Burt, T., and Williams, P. J.: Hydraulic conductivity in frozen soils, *Earth Surface Processes*, 1, 349-360,  
479 10.1002/esp.3290010404, 1976.

480 Campbell, G. S.: *Soil physics with BASIC: transport models for soil-plant systems*, Elsevier, Amsterdam,  
481 1985.

482 Cheng, Q., Xu, Q., Cheng, X., Yu, S., Wang, Z., Sun, Y., Yan, X., and Jones, S. B.: In-situ estimation of  
483 unsaturated hydraulic conductivity in freezing soil using improved field data and inverse numerical modeling,  
484 *Agr Forest Meteorol*, 279, 107746, 10.1016/j.agrformet.2019.107746, 2019.

485 Cortis, A., and Berkowitz, B.: Anomalous transport in “classical” soil and sand columns, *Soil Sci Soc Am*  
486 *J*, 68, 1539-1548, 10.2136/sssaj2004.1539, 2004.

487 Daniel, Stadler, and, Hannes, Flühler, and, Per-Erik, and Jansson: Modelling vertical and lateral water flow  
488 in frozen and sloped forest soil plots, *Cold Regions Science & Technology*, 10.1016/S0165-232X(97)00017-7,  
489 1997.

490 Demand, D., Selker, J. S., and Weiler, M.: Influences of macropores on infiltration into seasonally frozen  
491 soil, *Vadose Zone J*, 18, 1-14, 10.2136/vzj2018.08.0147, 2019.

492 Espeby, B.: Tracing the origin of natural waters in a glacial till slope during snowmelt, *J Hydrol*, 118, 107-  
493 127, 10.1016/0022-1694(90)90253-T, 1990.

494 Flerchinger, G. N., and Saxton, K. E.: *Simultaneous Heat and Water Model of a Freezing Snow-Residue-*  
495 *Soil System I. Theory and Development*, American Society of Agricultural Engineers, 10.13031/2013.31041,

496 1989.

497 Fouli, Y., Cade-Menun, B. J., and Cutforth, H. W.: Freeze–thaw cycles and soil water content effects on  
498 infiltration rate of three Saskatchewan soils, *Can J Soil Sci*, 93, 485-496, 10.4141/CJSS2012-060, 2013.

499 Fu, Q., Zhao, H., Li, T., Hou, R., Liu, D., Ji, Y., Zhou, Z., and Yang, L.: Effects of biochar addition on soil  
500 hydraulic properties before and after freezing-thawing, *Catena*, 176, 112-124, 10.1016/j.catena.2019.01.008,  
501 2019.

502 Gao, B., Yang, D., Qin, Y., Wang, Y., Li, H., Zhang, Y., and Zhang, T.: Change in frozen soils and its effect  
503 on regional hydrology, upper Heihe basin, northeastern Qinghai-Tibetan Plateau, *Cryosphere*, 12, 657-673,  
504 2018.

505 Gao, H., and Shao, M.: Effects of temperature changes on soil hydraulic properties, *Soil Till Res*, 153,  
506 10.1016/j.still.2015.05.003, 2015.

507 Gardner, W.: Some steady-state solutions of the unsaturated moisture flow equation with application to  
508 evaporation from a water table, *Soil Sci*, 85, 228-232, 10.1097/00010694-195804000-00006, 1958.

509 Granger, R. J., Gray, D. M., and Dyck, G. E.: Snowmelt infiltration to frozen Prairie soils, *Can J Earth Sci*,  
510 21, 669-677, 10.1139/e84-073, 1984.

511 Grevers, M., JONG, E. D., and St. Arnaud, R.: The characterization of soil macroporosity with CT  
512 scanning, *Can J Soil Sci*, 69, 629-637, 10.4141/cjss89-062, 1989.

513 Harlan, R.: Analysis of coupled heat - fluid transport in partially frozen soil, *Water Resour Res*, 9, 1314-  
514 1323, 10.1029/WR009i005p01314, 1973.

515 Hayashi, M., Kamp, G. V. D., and Schmidt, R.: Focused infiltration of snowmelt water in partially frozen  
516 soil under small depressions, *J Hydrol*, 270, 214-229, 10.1016/S0022-1694(02)00287-1, 2003.

517 Hayashi, M.: *The Cold Vadose Zone: Hydrological and Ecological Significance of Frozen-Soil Processes*,

518 Vadose Zone J, 12, 10.2136/vzj2013.03.0064, 2013.

519 Hussen, A., and Warrick, A.: Alternative analyses of hydraulic data from disc tension infiltrometers, Water  
520 Resour Res, 29, 4103-4108, 10.1029/93WR02404, 1993.

521 Jarvis, N.: A review of non - equilibrium water flow and solute transport in soil macropores: Principles,  
522 controlling factors and consequences for water quality, Eur J Soil Sci, 58, 523-546, 10.1111/j.1365-  
523 2389.2007.00915.x, 2007.

524 ~~Jarvis, N., Koestel, J., and Larsbo, M.: Understanding Preferential Flow in the Vadose Zone: Recent  
525 Advances and Future Prospects, Vadose Zone J, 15, 10.2136/vzj2016.09.0075, 2016.~~

526 Kamp, G. v. d., Hayashi, M., and Gallén, D.: Comparing the hydrology of grassed and cultivated  
527 catchments in the semi-arid Canadian prairies, Hydrol Process, 10.1002/hyp.1157, 2003.

528 Konrad, J.-M., and Morgenstern, N. R.: A mechanistic theory of ice lens formation in fine-grained soils,  
529 Can Geotech J, 17, 473-486, 10.1139/t80-056, 1980.

530 Lavelle, P., Decaëns, T., Aubert, M., Barot, S. b., Blouin, M., Bureau, F., Margerie, P., Mora, P., and Rossi,  
531 J.-P.: Soil invertebrates and ecosystem services, Eur J Soil Biol, 42, S3-S15, 10.1016/j.ejsobi.2006.10.002, 2006.

532 Lewis, J., and Sjöstrom, J.: Optimizing the experimental design of soil columns in saturated and  
533 unsaturated transport experiments, J Contam Hydrol, 115, 1-13, 2010.

534 Lipiec, J., Kuś, J., Słowińska-Jurkiewicz, A., and Nosalewicz, A.: Soil porosity and water infiltration as  
535 influenced by tillage methods, Soil and Tillage research, 89, 210-220, 10.1016/j.still.2005.07.012, 2006.

536 Lu, N., and Likos, W. J.: Unsaturated soil mechanics, Wiley, Hoboken, 2004.

537 Lundin, L.-C.: Hydraulic properties in an operational model of frozen soil, J Hydrol, 118, 289-310,  
538 10.1016/0022-1694(90)90264-X, 1990.

539 Luxmoore, R.: Micro-, meso-, and macroporosity of soil, Soil Sci Soc Am J, 45, 671-672,

540 10.2136/sssaj1981.03615995004500030051x, 1981.

541 McCauley, C. A., White, D. M., Lilly, M. R., and Nyman, D. M.: A comparison of hydraulic conductivities,  
542 permeabilities and infiltration rates in frozen and unfrozen soils, *Cold Reg. Sci. Technol*, 34, 117-125,  
543 10.1016/S0165-232X(01)00064-7, 2002.

544 Mohammed, A. A., Kurylyk, B. L., Cey, E. E., and Hayashi, M.: Snowmelt infiltration and macropore flow  
545 in frozen soils: Overview, knowledge gaps, and a conceptual framework, *Vadose Zone J*, 17, 1-15,  
546 10.2136/vzj2018.04.0084, 2018.

547 [Mohammed, A. A., Pavlovskii, I., Cey, E. E., and Hayashi, M.: Effects of preferential flow on snowmelt](#)  
548 [partitioning and groundwater recharge in frozen soils, \*Hydrol Earth Syst Sc\*, 23, 5017-5031, 10.5194/hess-23-](#)  
549 [5017-2019, 2019.](#)

550 [Nimmo, J. R.: Theory for Source-Responsive and Free-Surface Film Modeling of Unsaturated Flow,](#)  
551 [Vadose Zone J, 9, 295-306, 10.2136/vzj2009.0085, 2010.](#)

552 [Nimmo, J. R.: Preferential flow occurs in unsaturated conditions, \*Hydrol Process\*, 26, 786-789,](#)  
553 [10.1002/hyp.8380, 2012.](#)

554 Nixon, J.: Discrete ice lens theory for frost heave in soils, *Can Geotech J*, 28, 843-859, 10.1139/t91-102,  
555 1991.

556 Oswald, S., Kinzelbach, W., Greiner, A., and Brix, G.: Observation of flow and transport processes in  
557 artificial porous media via magnetic resonance imaging in three dimensions, *Geoderma*, 80, 417-429,  
558 10.1016/S0016-7061(97)00064-5, 1997.

559 Oztas, T., and Fayetorbay, F.: Effect of freezing and thawing processes on soil aggregate stability, *Catena*,  
560 52, 1-8, 10.1016/S0341-8162(02)00177-7, 2003.

561 Peng, X., Frauenfeld, O. W., Cao, B., Wang, K., Wang, H., Su, H., Huang, Z., Yue, D., and Zhang, T.:

562 Response of changes in seasonal soil freeze/thaw state to climate change from 1950 to 2010 across china,  
563 Journal of Geophysical Research Earth Surface, 10.1002/2016JF003876, 2016.

564 Perroux, K. M., and White, I.: Designs for Disc Permeameters, Soil Sci Soc Am J, 52, 1205-1215,  
565 10.2136/sssaj1988.03615995005200050001x, 1988.

566 Pittman, F., Mohammed, A., and Cey, E.: Effects of antecedent moisture and macroporosity on infiltration  
567 and water flow in frozen soil, Hydrol Process, 34, 795-809, 10.1002/hyp.13629, 2020.

568 Smith, M.: Observations of soil freezing and frost heave at Inuvik, Northwest Territories, Canada, Can J  
569 Earth Sci, 22, 283-290, 10.1016/0148-9062(85)90073-7, 1985.

570 Spaans, E. J.: The soil freezing characteristic: Its measurement and similarity to the soil moisture  
571 characteristic, 1994.

572 Spaans, E. J., and Baker, J. M.: The soil freezing characteristic: Its measurement and similarity to the soil  
573 moisture characteristic, Soil Sci Soc Am J, 60, 13-19, 10.2136/sssaj1996.03615995006000010005x, 1996.

574 Stadler, D., Stähli, M., Aeby, P., and Flüeler, H.: Dye tracing and image analysis for quantifying water  
575 infiltration into frozen soils, Soil Sci Soc Am J, 64, 505-516, 10.2136/sssaj2000.642505x, 2000.

576 Stähli, M., Bayard, D., Wydler, H., and Flüeler, H.: Snowmelt Infiltration into Alpine Soils Visualized by  
577 Dye Tracer Technique, Arctic Antarctic & Alpine Research, 36, 128-135, 10.1657/1523-  
578 0430(2004)036[0128:SIASV]2.0.CO;2, 2004.

579 Taina, I. A., Heck, R. J., Deen, W., and Ma, E. Y.: Quantification of freeze–thaw related structure in  
580 cultivated topsoils using X-ray computer tomography, Can J Soil Sci, 93, 533-553, 10.4141/CJSS2012-044,  
581 2013.

582 Tarnawski, V. R., and Wagner, B.: On the prediction of hydraulic conductivity of frozen soils, Can Geotech  
583 J, 33, 176-180, 10.1139/t96-033, 1996.

584 Wang, D., Yates, S., and Ernst, F.: Determining soil hydraulic properties using tension infiltrometers, time  
585 domain reflectometry, and tensiometers, *Soil Sci Soc Am J*, 62, 318-325,  
586 10.2136/sssaj1998.03615995006200020004x 1998.

587 Wang, X., Chen, R., Liu, G., Yang, Y., Song, Y., Liu, J., Liu, Z., Han, C., Liu, X., Guo, S., Wang, L., and  
588 Zheng, Q.: Spatial distributions and temporal variations of the near-surface soil freeze state across China under  
589 climate change, *Global Planet Change*, 172, 150-158, 10.1016/j.gloplacha.2018.09.016, 2019.

590 Watanabe, K., and Flury, M.: Capillary bundle model of hydraulic conductivity for frozen soil, *Water*  
591 *Resour Res*, 44, 10.1029/2008WR007012, 2008.

592 Watanabe, K., and Wake, T.: Hydraulic conductivity in frozen unsaturated soil, *Proceedings of the 9th*  
593 *International Conference on Permafrost*, 2008, 1927-1932,

594 Watanabe, K., Kito, T., Dun, S., Wu, J. Q., Greer, R. C., and Flury, M.: Water infiltration into a frozen soil  
595 with simultaneous melting of the frozen layer, *Vadose Zone J*, 12, vzj2011.0188, 10.2136/vzj2011.0188, 2013.

596 Watanabe, K., and Kugisaki, Y.: Effect of macropores on soil freezing and thawing with infiltration, *Hydrol*  
597 *Process*, 31, 270-278, 10.1002/hyp.10939, 2017.

598 Watanabe, K., and Osada, Y.: Simultaneous measurement of unfrozen water content and hydraulic  
599 conductivity of partially frozen soil near 0 C, *Cold Reg. Sci. Technol*, 142, 79-84,  
600 10.1016/j.coldregions.2017.08.002, 2017.

601 Watson, K., and Luxmoore, R.: Estimating macroporosity in a forest watershed by use of a tension  
602 infiltrometer, *Soil Sci Soc Am J*, 50, 578-582, 10.2136/sssaj1986.03615995005000030007x, 1986.

603 Williams, P., and Burt, T.: Measurement of hydraulic conductivity of frozen soils, *Can Geotech J*, 11, 647-  
604 650, 10.1139/t74-066, 1974.

605 Williams, P. J., and Smith, M. W.: *The frozen earth: fundamentals of geocryology*, Cambridge University



606 Press, 1989.

607 Wilson, G., and Luxmoore, R.: Infiltration, macroporosity, and mesoporosity distributions on two forested  
608 watersheds, *Soil Sci Soc Am J*, 52, 329-335, 10.2136/sssaj1988.03615995005200020005x, 1988.

609 Wooding, R.: Steady infiltration from a shallow circular pond, *Water Resour Res*, 4, 1259-1273,  
610 10.1029/WR004i006p01259, 1968.

611 Zhao, Y., Nishimura, T., Hill, R., and Miyazaki, T.: Determining hydraulic conductivity for air - filled  
612 porosity in an unsaturated frozen soil by the multistep outflow method, *Vadose Zone J*, 12, 1-10,  
613 10.2136/vzj2012.0061, 2013.